Dynamic Behavior of the Palazzo Lombardia Tower: Comparison of Numerical Models and Experimental Results

Alfredo Cigada[1]; Elena Mola[2]; Franco Mola[3]; Gianfranco Stella[4]; and Marcello Vanali[5]

Introduction

The Palazzo Lombardia project, the new seat for the Milan offices of the Lombardia Region, is one of the most significant in the Italian panorama of the last few decades, setting the record for the tallest building in Italy (at 161.30 m), according to the definitions provided by the Council of Tall Buildings and Urban Habitat (CTBUH). The building, with its distinctive architectural features, certainly is set to strongly mark Milan's skyline for years to come.

The complex is made up of five lower buildings (about 40 m high, called Cores 2–6), surrounding the high-rise Tower (Core 1), which scored the aforementioned height record in Italy. The complex's sinuous interweaving strands recall the mountains, valleys, and rivers of the Lombardia region. The curvilinear forms largely used in the architectural design, and clearly visible in the facades of all the buildings, are adaptable to changing functional requirements and are receptive to the region's evolving organizational structure.

[1]Dept. of Mechanical Engineering, Polytechnic Univ. of Milan, 20156 Milan, Italy.

[2]ECSD Engineering, Via Goldoni 22, 20129 Milan, Italy.

[3]Dept. of Structural Engineering, Polytechnic Univ. of Milan, 20132 Milan, Italy.

[4]CAD DataConsult, Via Cadolini 4, 20137 Milan, Italy.

[5]Dept. of Industrial Engineering, Univ. of Parma, 43124 Parma, Italy (corresponding author). E-mail: marcello.vanali@unipr.it

Note. This manuscript was submitted on June 21, 2012; approved on January 2, 2013; published online on May 15, 2014. Discussion period open until November 1, 2014; separate discussions must be submitted for individual papers.

The curvilinear shapes of the buildings, while having a very strong aesthetic impact, also are reflected in the irregular planwise configuration of the complex, which, at its center, defines an inner covered public plaza having an area of approximately 4,200 m^2. This is covered by a steel truss system supporting transparent Texlon ethylene-cotetrafluoroethylene (ETFE) cushions. In Fig. 1, the six buildings (Cores 1–6) that make up the complex are visible.

The structural system is made entirely of RC load-bearing elements, except for the auditorium area in Core 4 and the Velarium on top of Core 1, a 3-story belvedere area to be used for official public purposes and rented out for private events. For these two parts, structural steel was employed.

Because of the strategic importance of the building and according to the Italian building code requirements, (Consiglio Superiore dei Lavori Pubblici 2008), a detailed analysis of the dynamic behavior was needed to assess structural response to earthquakes. Moreover, a detailed FEM model was needed to prevent any possible vibration serviceability issue according to international standards and guidance [ISO 1997; ISO 2003; British Standards Institution (BSI) 1990; Institution of Structural Engineers 2008; Canadian Commission on Building and Fire Codes 2006]. Consequently, the numerical FE model was implemented for the most sensitive building part, Core 1, to have the possibility to predict its dynamic response. Further, a series of experimental tests were planned and executed to validate the model results and possibly perform a first model-updating attempt (Cigada et al. 2011). The estimated dynamic parameters will be used as a reference for future structural health–monitoring activities (Brownjohn 2007), based on dynamic measurements too.

It is a well-known fact that, among the several health-assessment methods available in the literature, the vibration-based, damage-identification technique seems to be one of the most promising families. Many reviews have been published, where several methods

Fig. 1. Palazzo Lombardia: the architectural project (photo by Piero Mollica, Infrastrutture Lombarde S.p.A Archive; reproduced with permission)

presented in the literature are classified as a function of the exploited monitoring feature and their performances described (Doebling et al. 1996, 1998; Sohn et al. 2004; Carden 2004; Fan and Qiao 2010).

The results given in the cited references highlighted how the structure-vibration feature could be used to define correctly the level of structural damage, and stressed the reliability of this approach to structural health monitoring (SHM).

The integrity of civil infrastructures can be evaluated by extracting information from their dynamic-response measurements. The idea is that damage changes the physical properties and, consequently, causes detectable changes in modal properties. Therefore, modal parameters are one of the most used indicators in the literature to represent the structural behavior and to assess the health condition accordingly (Salawu 1997; Huth et al. 2005). Modal-domain methods are gaining wide attention among all the reported monitoring techniques, because modal properties have their own physical meanings and are easier to interpret than abstract features obtained by time- or frequency-domain processing. All these methods have one thing in common: they compare the current identified modal parameters with a set of benchmark values, representing the structure in its initial healthy condition. Thus, they all need an initial set of modal parameters and a reliable identification method to assess the parameter evolution. The modal-parameter evolution then is studied and interpreted by means of numerical models to identify the origin of the identified changes (Teughels and De Roeck 2004; Cigada et al. 2008a). This is the reason why a validated numerical model represents an important tool for SHM purposes.

The initial modal-parameter estimation, and generally any modal analysis, can be performed by two different approaches: (1) applying a known excitation (by means of a hydraulic actuator, vibrodyne, etc.), or (2) exploiting the unknown forcing caused by environmental load sources (e.g., traffic and wind). The former is called experimental modal analysis (EMA; Ewins 2001), whereas the latter is known as operational modal analysis (OMA; Farrar 1997; Cigada et al. 2008b, Caprioli et al. 2009). While both methods are suitable for an initial test, the need for an external excitation in the EMA case makes OMA tests preferable in a continuous SHM case.

However, EMA tests give more accurate results, so they are useful to define the benchmark values of the modal properties and to perform the initial model updating. Normally carried out once a structure is built, EMA tests provide the initial picture of the as-built structure. EMA generally guarantees complete control of the test conditions. For example, the excitation level may be defined for every analysis, and the results, obtained with different forcing amplitudes, can be compared with one another. Moreover, it is possible to keep a detailed record of all the external influencing parameters, such as temperature and humidity. Nonetheless, EMA is expensive and time consuming; a proper actuator has to be placed on the structure, making it impossible to perform a continuous monitoring of the modal parameter evolution.

On the other hand, OMA does not allow the same level of control on the influencing parameters to be attained, as some of them are not even measurable. While external variables, such as temperature and humidity, can be measured, there are other uncertain sources that are not controllable. For example, the exact excitation input of the system is not known, only some assumptions can be made. Notably, these assumptions can be misleading, because the excitation input due to sources like traffic, wind, or people walking on the structure does not always strictly fulfill OMA requirements (Mohanty and Rixen 2004). Huth et al. (2005) showed the advantages of using output-only system identification, but the results stress how the modal parameter estimation is affected deeply by the environmental conditions, as shown in other references (Cornwell et al. 1999). Indeed, the challenge of today's research is the definition of damage-identification features independent of humidity and temperature, and being aware of all the uncertainties in the parameter identification (Cattaneo et al. 2010, 2011; Pintelon et al. 2007; El Kafafy et al. 2012). However, OMA is more cost effective and easier to perform. The only needs are a proper number of transducers placed on the structure and a continuous data-acquisition system. By exploiting this setup, a continuous monitoring of the modal parameters can be performed (Cigada et al. 2008c, 2010; Vanali and Cigada 2009).

It must be stated that OMA results are strengthened by a direct comparison with the EMA ones, providing an experimental benchmark of their reliability and to assess the structural behavior evolution. A good agreement between EMA and OMA is required to guarantee that the fundamental assumptions of OMA are complied with by the tested structure and its environment, and to identify possible disturbances that will lead to erroneous mode identifications.

In this paper, the model description, results, and the experimental tests are presented together. A comparison is performed between the numerical modal-parameter prediction and the experimentally derived structural ones. At first, the structure itself is described and some of the design choices are discussed. The FE model is then introduced, together with the description of the basic modeling assumptions. Following this, the experimental setup and the experimental tests are presented, and a final comparison with the FE model results is given.

The results shown in the paper set a benchmark for the future health monitoring of the building, which also will be based on the evaluation of the modal-parameter evolution, among other indicators.

Description of the Structure and Design Choices

A thorough description of the structural features of the complex and a discussion of the reasons behind the basic conceptual design choices are provided elsewhere (Mola 2010). In this paper, only a few highlights, most of them regarding Core 1, are reported, with the purpose of better clarifying the modeling assumptions enforced in the implementation of the FE model of Core 1.

The load-bearing elements of Core 1 are made entirely of RC: the lateral load-bearing capacity is provided fully by a central stairway core, whereas the vertical structural elements are circular columns with varying cross sections and diameters ranging between 120 and 65 cm.

The slabs are different along the height of the building: the underground floors are interconnected with those of the lower cores. Also, from the ground floor, and up to the top slab of the lower buildings (i.e., at a height of about 40 m), the slabs are interconnected. From level 13 to the top, the floor surface reduces to that of Core 1 only.

The slabs of Core 1, starting from the 13th floor, are 35 cm thick RC structural systems (usually referred to as bubble decks) behaving as plates. The reduction of weight is obtained by inserting high-density polyethylene (PEHD) spheres with a diameter of 270 mm in the slab, holding them in place during casting by means of retaining rebar cages, in addition to the usual bidirectional structural rebar layers (Fig. 2).

The use of this construction technology generated two advantages from a structural point of view: (1) improving the seismic response, because these reduced-weight slabs weigh up to 20% less than their fully cast in situ counterparts; and (2) speeding up the construction phase.

In fact, an unusual structural system was adopted to build Core 1: the vertical RC elements were cast into steel formworks. The encasing elements were holed so that slab rebar and concrete could pass through, thus making the column-to-slab joints completely effective in bearing lateral load-induced moments. The slabs and columns are shown in Figs. 3(a and b), respectively. The use of steel encasing for the vertical elements allowed simultaneous casting of up to three floors. In this structural system, the lightweight bubble-deck slabs exhibit the behavior of a continuous plate on point supports (the columns) and continuous support (the walls of the core). The peculiar features of the column-to-slab joints were an aspect of interest and investigation when the FE model was created, as detailed subsequently.

Another significant feature affecting the global modal properties of the structure and, as a consequence, the FE model results, is in the foundations. The foundations of Core 1 are made of a slab with a thickness ranging between 2 and 4 m. Under the slab, the ground was injected with compacting grout columns, having a diameter of 1.5 m, spacing between 3 and 4 m, and depth between 14 and 22 m. Self-compacting concrete was used to cast the lower layer of the slab, owing to the strong rebar congestion, then normal concrete was used for the remaining depth. The two layers were interconnected by means of vertical steel bars purposely distributed in the slab. All the steel bars were joined by means of steel couplers.

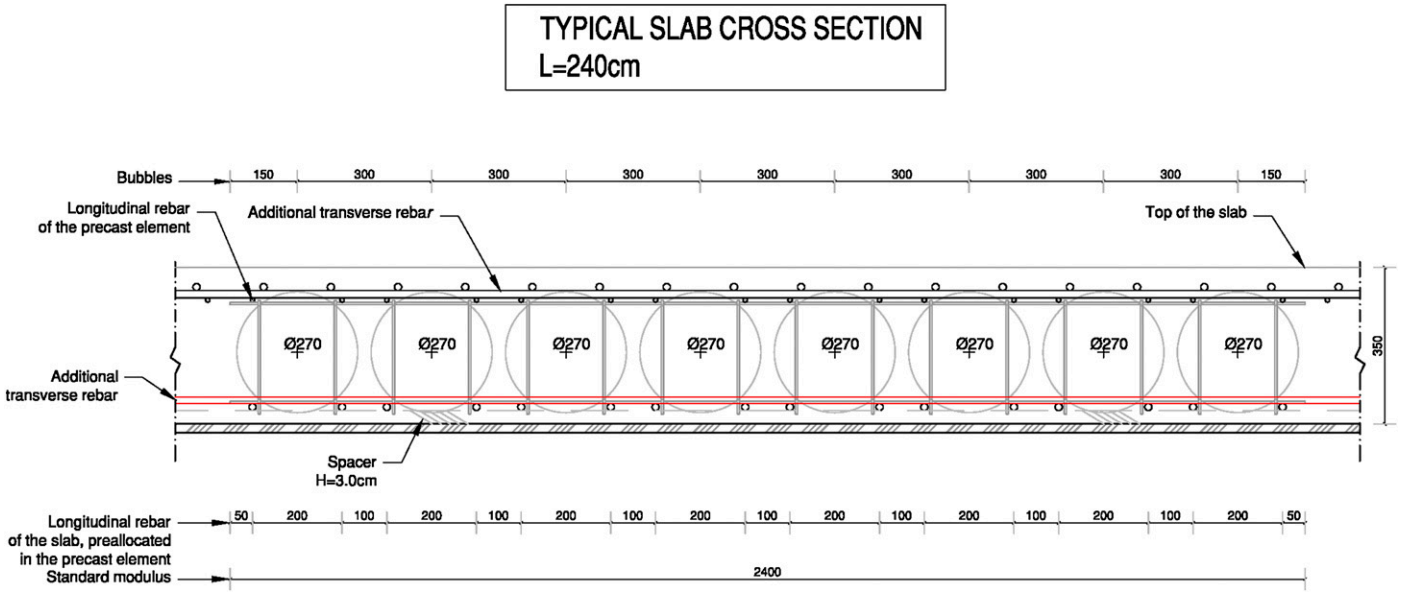

Fig. 2. Slab section

Fig. 3. Structural details (photos by Piero Mollica, Infrastrutture Lombarde S.p.A Archive; reproduced with permission): (a) bubble decks in Core 1; (b) steel encasing for columns of Core 1

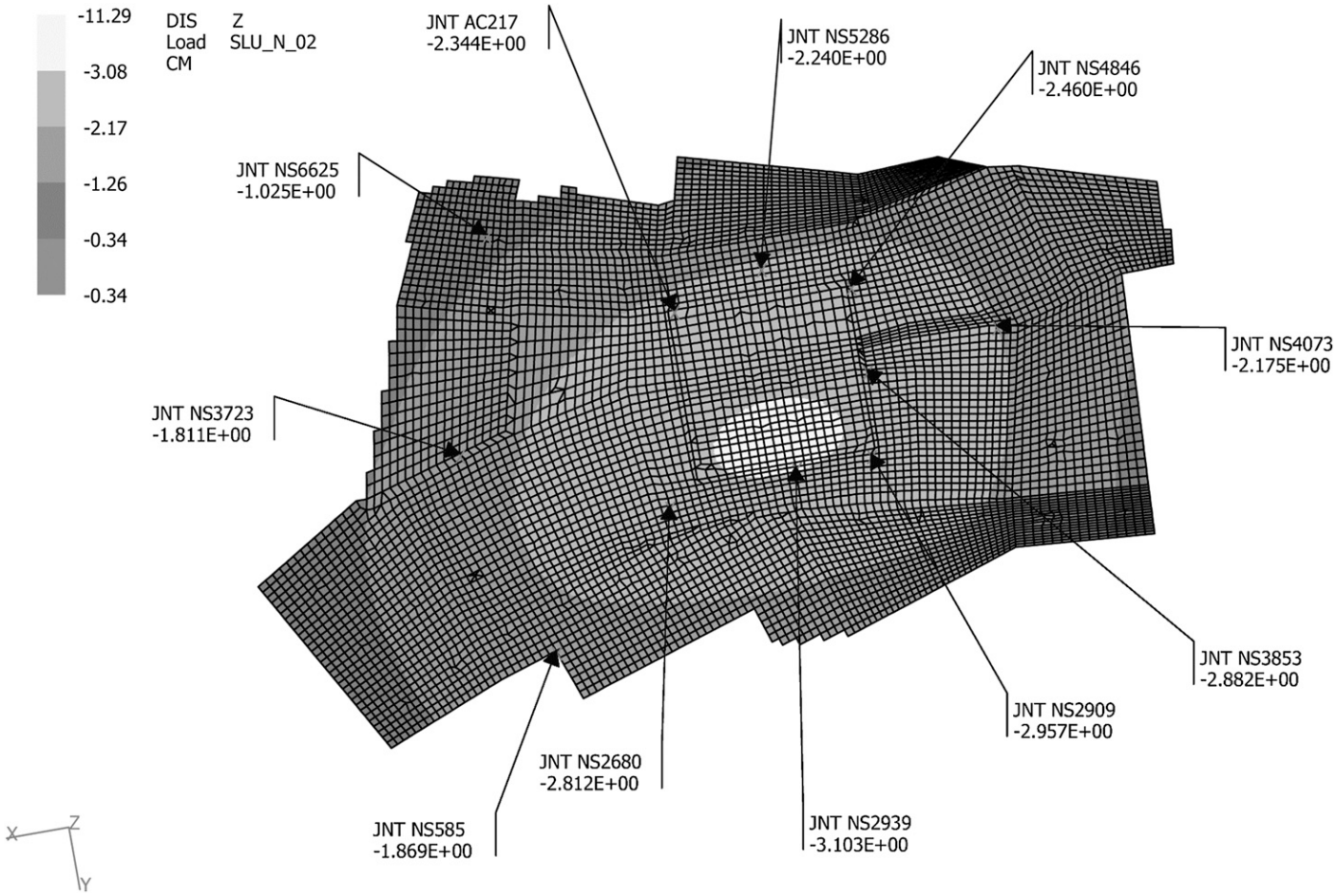

Fig. 4. Foundation slab analysis: distribution of soil pressure

The foundation slab was initially analyzed as a plate on an elastic surface, according to Winkler's model, for predimensioning purposes. Structural analysis was carried out on a three-dimensional (3D) shell-element model representing the slab, with different subgrade coefficient values ranging between 0.5×10^{-3} and $2.5 \times 10^{-3}\,\mathrm{N/mm^3}$.

In Fig. 4, the soil pressure resulting from the analysis is represented. The highest values of such pressure, about 0.5 MPa, were distributed in the central part of the slabs, below Core 1, which led to an increase in the slab thickness in this area, so that differential displacements between the foundation of the inner core of the tower and those of the columns could be limited.

When implementing the global FE model, the foundation slab was included. At first, the stiffness of the foundation was assumed as the one computed by means of the separate submodel; in a later phase, different subgrade coefficient values were assumed in the model to test the sensitivity of the final results to this parameter.

FE Model: Features and Analysis

The FE model of Core 1 was implemented using *GT STRUDL 30*, commercial software for structural analysis, to run both static and dynamic analyses.

Static analyses were meant for the validation of the conceptual design and the dimensioning of the structural elements; the optimization of the performance of the structural elements, both in the service limit state and at ultimate, was pursued by means of iterative analyses.

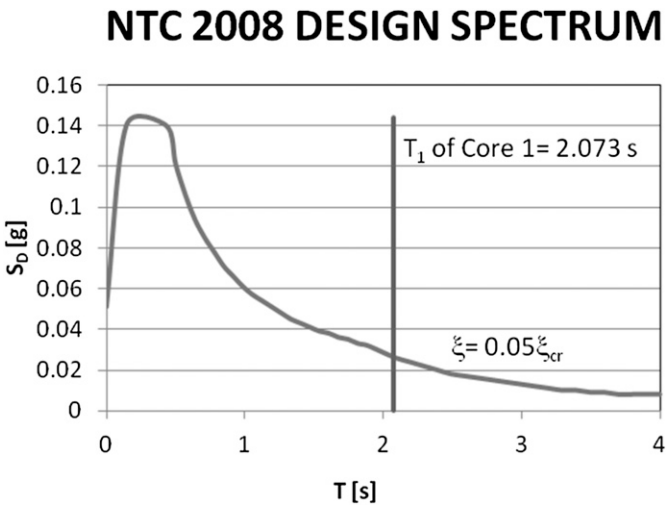

Fig. 5. Norme tecniche delle costruzioni (NTC) spectrum and fundamental period

Given the inherent flexibility of the structure, its first modal period turned out to be well in the tail section of the EC8-type design spectrum enforced in the Italian building code (Consiglio Superiore dei Lavori Pubblici 2008) for modal-response spectrum analysis (Fig. 5). On the other hand, given the very wide surfaces exposed to wind pressure, static analyses confirmed that the most critical

loading condition for lateral load-bearing capacity was owing to the wind, so that, for dimensioning purposes, the strongest wind in the exercise-limit state was used.

To derive the modal features of the structure, a linear dynamic modal analysis was then carried out. The main purpose of the analysis was to provide accurate numerical predictions of the modal response of the building, which would be compared with the series of dynamic excitation tests that were to be run on the as-built structure as a prerequisite for its final validation.

The global FE model was implemented assuming the nominal design properties of materials and of the ground and accurately describing both the global geometry and the local features of the different structural elements. The 27 basic loading conditions and five loading combinations implemented in the model allowed it to reproduce effectively the real mass distribution of the structure in the various construction stages and service-life conditions.

It was deemed important to properly model the slab-to-column connections and, in general, to replicate the behavior of the slabs of the Tower in the closest possible way. In fact, the global stiffness of the model was affected strongly by the assumed stiffness of the column-to-slab connections. The presence of the columns, having large cross sections (from 60 up to 120 cm at the bottom), reduced the flexural deformation of the slabs, with a restraining effect that needed to be quantified and reproduced correctly in the FE model. For this reason, the so-called bubble-deck slabs described previously (i.e., cast in situ RC slabs lightened by means of poliethylene spheres) were modeled by means of shell elements with an equivalent thickness to provide the correct flexural stiffness [Figs. 6(a and b)].

To investigate the sensitivity of the global modal properties to the effective stiffness distribution in slabs, two meshing options were explored, imposing different restraints to the joints closest to the columns. The first mesh did not take into account the stiffening effect of the effective cross sections of the columns on the joints of the slab mesh; the second mesh did take into account the presence of cross sections of the columns by means of an increased thickness of the slab elements where each column was present and in its immediate vicinity. The increase in thickness was quantified by means of a service submodel focusing on one single floor, analyzed with a more-refined mesh.

Modal dynamic analyses were carried out assuming linear elastic behavior of materials, because it was expected that the experimental excitation provided to the structure during the tests would have to be well in the elastic range of the response, being produced by the wind or purposely designed exciters.

It is well known that the modal properties depend on the actual material properties; in particular, the actual elastic modulus of concrete, which is used to determine the stiffness matrix, depends in turn on the type of concrete and its compressive strength. For this reason, when using the nominal design properties of materials in the FE model instead of the as-built ones, a margin of error remains. In the case of Core 1, the results of the compressive strength tests on cubes extracted during construction were available; thus, a mean value of the compressive strength was derived for the different structural elements and, from this, by applying the Model Code 90 [Fédération International de la Précontrainte (CEB/FIP) 1993] formulation (1), the corresponding elastic modulus was computed

$$E_c(t') = \beta_E(t') \cdot E_{c,28} \tag{1}$$

where

$$\beta_E(t') = [\beta_{cc}(t)]^{0.5}$$

$$\beta_{cc}(t) = \exp\left\{ s\left[1 - \left(\frac{28}{t/t_1}\right)^{1/2}\right]\right\}$$

and $t_1 = 1$ day; $s = 0.25$ (normal concrete); $E_{c,28} = E_{c0}[(f_{ck} + \Delta f)/f_{cm0}]^{1/3}$; $E_{c0} = 2.15 \times 10^4$ MPa; f_{ck} = characteristic strength (MPa); $\Delta f = 8$ MPa; and $f_{cm0} = 10$ MPa. Two different modeling assumptions were then made to investigate the sensitivity of the modal properties to a change in the material properties: (1) the nominal design properties of all the employed materials were implemented in the model, and then, (2) the actual elastic moduli derived from the experimental compressive strength were implemented for each class or group of elements. The results proved that the sensitivity of the first eigenfrequencies and eigenvectors to this parameter was much lower than that to a mesh refinement; thus, the design properties of materials were assumed in all the subsequent analyses.

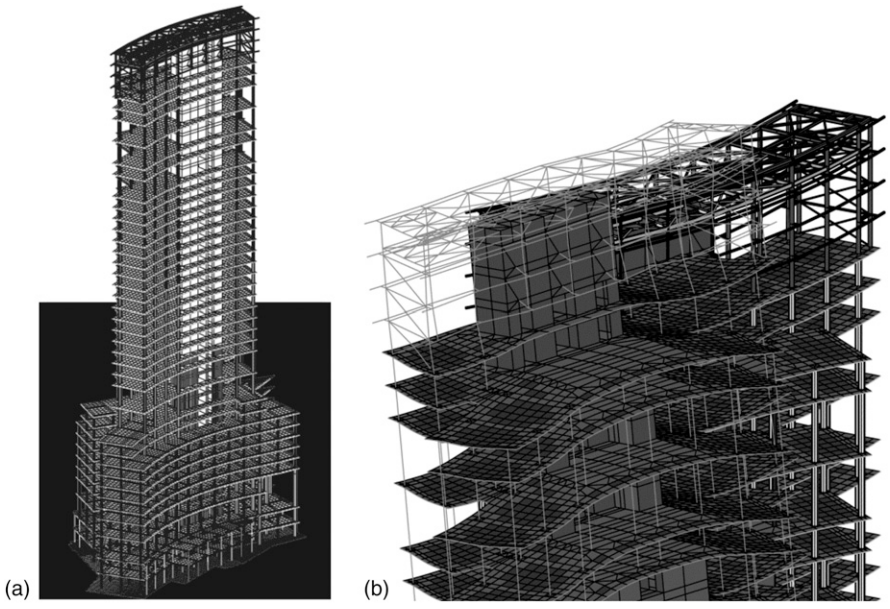

Fig. 6. FE model in *GT STRUDL* (model screen shots): (a) global view; (b) partial view of core elements, slab elements, and steel truss elements

Modal frequencies and modal shapes not only depend on the stiffness distribution (both of cross section inertiae and elastic moduli), but also on the actual mass distribution—both the structural masses and those of the loads that were already present when the tests were conducted, the latter assumed to be just a fraction of the design loads. Because the experimental dynamic excitation tests were done at the end of construction but before the whole static permanent loading was put in place, it was necessary to compute the actual masses present on the structure at the time of the tests. For the final simulations, it was computed that a fraction of 20% of the permanent loading would be present; in fact, only the floors and the external glass facade were present at the time of the tests.

Finally, as for the foundation properties, a subgrade coefficient value of $2.0 \times 10^{-3}\,\mathrm{N/mm^3}$ was assumed; this was the design value used in the predimensioning analyses run separately on the foundations alone, and it proved to be the value of this parameter providing the modal response that best matched the experimentally derived one.

The *GT STRUDL* software, one of the longest established structural analysis softwares currently available, couples high reliability of the results with strongly reduced computational times. The total computational time for the modal analyses of the Tower model was 5 min if the optimized processor was employed and 12 min if the standard processor was used.

Experimental Tests: Features and Results

Dynamic testing is increasingly important as a valuable tool that provides a validation to refine and eventually update numerical simulation models and gives information about the response to an external stimulus (e.g., wind or an earthquake).

It is commonly acknowledged that static numerical models need a further refinement step to account for dynamic features. Mass distribution and stiffness only can be computed with given uncertainty levels, as discussed previously, and damping coefficients are hard to estimate theoretically and sometimes affected by strong nonlinear structural behaviors. A check on both static and dynamic behavior can help narrow this uncertainty. Another key goal is creating the basis for a proper permanent monitoring. In the case of Palazzo Lombardia, given its importance, a series of dynamic excitation tests were deemed a mandatory prerequisite for the final design validation.

Test Setup and First Operational Modal Analysis Results

The main problems in testing a skyscraper are properly predicting the mode shapes, affixing sensors in the right positions, and having the certainty of a proper input to excite the structure and produce a meaningful vibration, enough to be measured.

As previously mentioned, in the Palazzo Lombardia complex, Core 1 is by far the most critical structure in terms of dynamic response; therefore, this building was the focus. The main global behavior of Core 1 is that of a cantilever beam, at least in a first approximation approach; as mentioned previously, the regular distribution of load-bearing elements in the floor plan made it easier to predict a regular and mostly uncoupled modal response. In fact, the numerical model provided an initial approximation of the expected vibration modes and frequencies that reasonably could be assumed as a confirmation of this behavior. To further confirm these assumptions, a short pretest exploiting ambient vibration was designed and executed. The idea was to exploit OMA (Farrar 1997; Cigada et al. 2008b) approaches to get a first experimental estimate of the natural frequencies and a rough idea of the associated mode shapes.

Three acceleration measurement positions were chosen on the Tower's 38th floor (the upper floor of the building), as shown in Fig. 7. As the main natural frequencies of interest were expected in the range of 0.1–2 Hz, piezo accelerometers PCB 393B12 (PCB Piezotronics, Depew, New York) were chosen, which are characterized by a 0.1–500 Hz bandwidth, 10 V/g sensitivity, $\pm 0.5g$ measurement range, and $12.7\,(\mu\mathrm{m/s^2})/\sqrt{\mathrm{Hz}}$ spectral noise in correspondence to 1 Hz. All the sensors were conditioned by a PCB integrated electronic piezoelectric unit with high-pass filtering at 0.1 Hz and acquired by means of a National Instruments (Austin, Texas) device equipped with 24-bit acquisition modules with antialiasing filter. Owing to data-acquisition system performances, a high sampling frequency was adopted (2,048 Hz).

Both accelerometers and data-acquisition systems had valid calibration certificates traceable to the NIST.

A part of the installed measurement system for the operational pretest is shown in Fig. 8 (data-collection unit and some accelerometers during the calibration phase).

The first test exploited ambient excitation for 1 week, considering wind and traffic as the unknown input. In addition to gauging the sensitivity of the structure to this excitation, this test also allowed for a first check on the identification of the first natural frequencies and

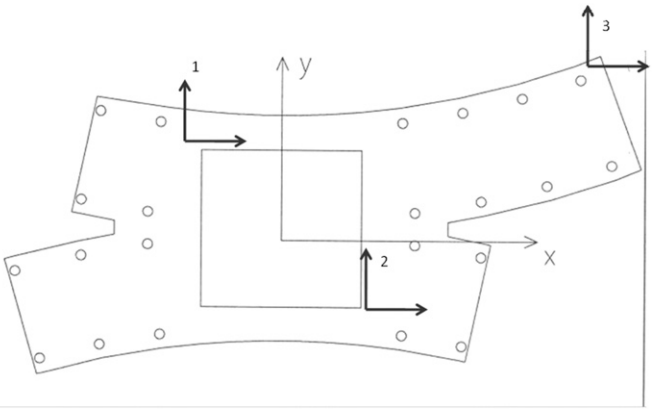

Fig. 7. Accelerometer positions on the 38th floor

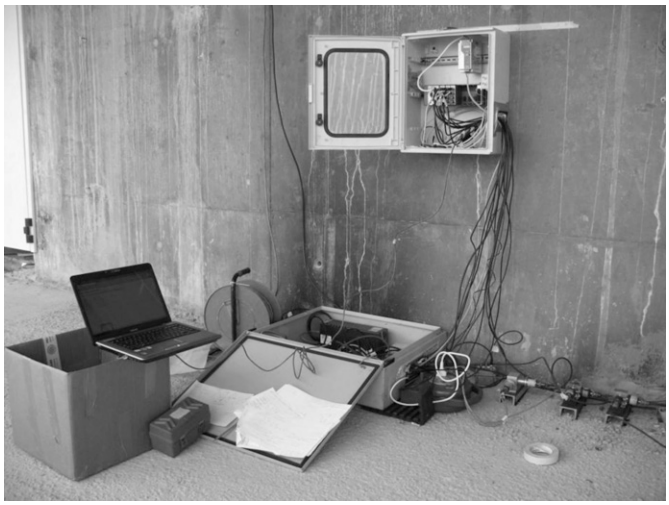

Fig. 8. Pretest operational setup on the building

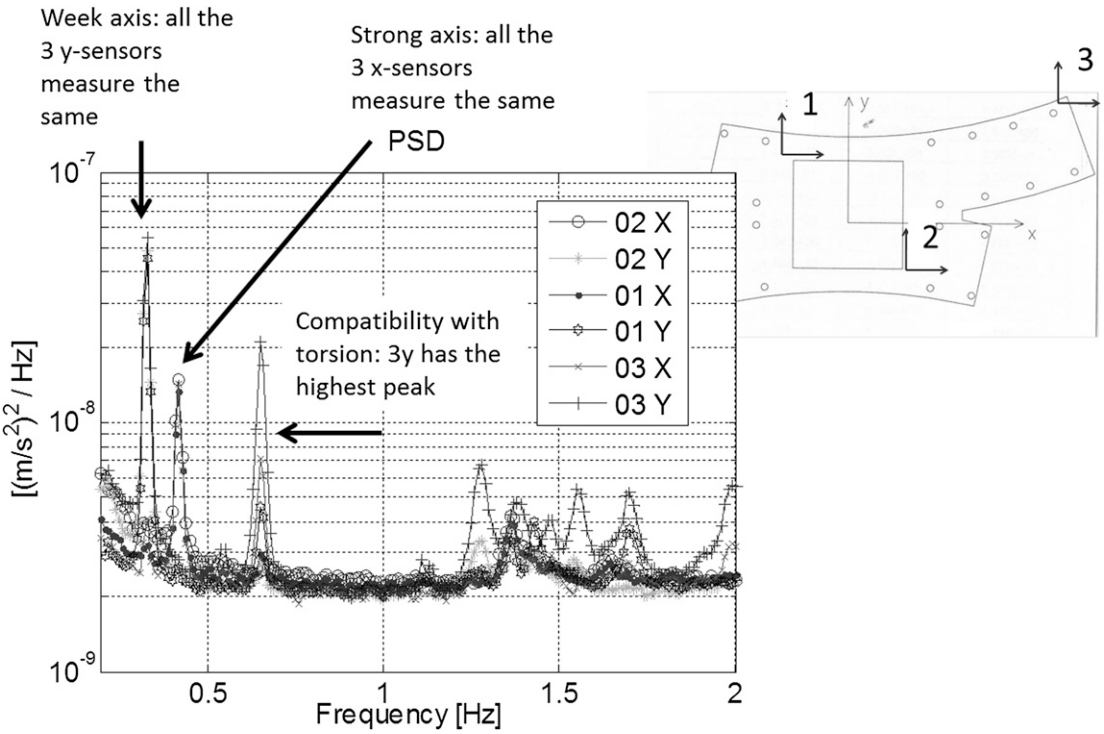

Fig. 9. Measured accelerations PSD at 38th floor (OMA test)

the related mode shapes. Even if the signal-to-noise ratio was less favorable in this kind of test, acquisition through the whole week allowed for an improvement in the output signals, obtained by averaging spectral quantities over numerous suitable time windows (D'Antona and Ferrero 2006; Bendat and Piersol 2000). The selected time windows were chosen to assure the reliability of the measured data, avoiding possible shocks and overloads.

Fig. 9 provides one of the outputs from these tests, in terms the power spectral density (PSD), averaged on a 24-h time window, for the measurement points on the 38th floor. Three main peaks are clear in the lowest frequency range: the 0.33 Hz mode shows all the weak-axis sensitive accelerometers measuring the same amplitude, justifying a flexural mode; the same applies to the 0.42 Hz mode, just exchanging the weak axis with the strong axis. The third peak, at 0.65 Hz, exhibits higher amplitudes as the distance from the main core increases, which is consistent with torsion. Any contribution at higher frequencies is not so easily detectable, having peaks close to the transducers noise floor: ambient excitation cannot input enough energy to excite higher modes. A summary of the OMA-identified values for the first three vibration modes using the polyreference least-squares frequency-domain algorithm (Peeters et al. 2005) is given in Table 1.

The estimated damping values showed a higher spread, being a function of the considered time windows within the testing week, which also is confirmed by literature results (Cattaneo et al. 2011; El Kafafy et al. 2012).

Forced Vibration Test Setup

On the basis of the numerical model outputs and the first operational results, the location of the forced test sensors was decided and the expected range of potential resonance frequencies was defined. Moreover, exploiting the rough damping estimate given by OMA and the numerical modal analysis results, a first approximation about the needed input to produce a measurable output was derived.

Table 1. Identified Modal Frequencies and Damping for the First Three Modes via OMA

Mode	Frequency (Hz)	Estimated damping (% RC)
1	0.33	1.8
2	0.42	2.2
3	0.65	1.6

The sensors were located on three different floor levels, the 21st, the 32nd, and the 38th, considered enough to identify the first vibration mode shapes (Fig. 10). Each floor was instrumented with two orthogonal-axis accelerometers in the horizontal plane, with four measurement points on each floor so that both flexural modes (strong and weak axis) and torsional modes could be identified.

While setting up the forced test, a rather windy day was experienced; ambient-vibration data were acquired and the relative PSD was estimated with a better signal-to-noise ratio compared with the previous ambient data, because measurement points across three floors already were available. The results from the first OMA measurement were strengthened by this new data set; moreover, a further confirmation of the previously predicted mode shapes was obtained. As an example, Fig. 11 refers to the weak-axis accelerations at different floors: for the first flexural mode, an increase in the acceleration peaks at different heights can be observed, as expected, and coherent with a cantilever first mode.

Concerning forced tests, one of the most important issues, when dealing with large structures having low natural frequencies, is providing an adequate energy input to guarantee a coherent structural response. It is well known how inertial exciters have problems in producing a meaningful force at low frequencies. The inertia force is the product between mass and acceleration; assuming the excitation to be harmonic, acceleration is low at low frequencies, as the peak acceleration is the displacement peak amplitude multiplied by the circular frequency squared. It comes out that high energies at low

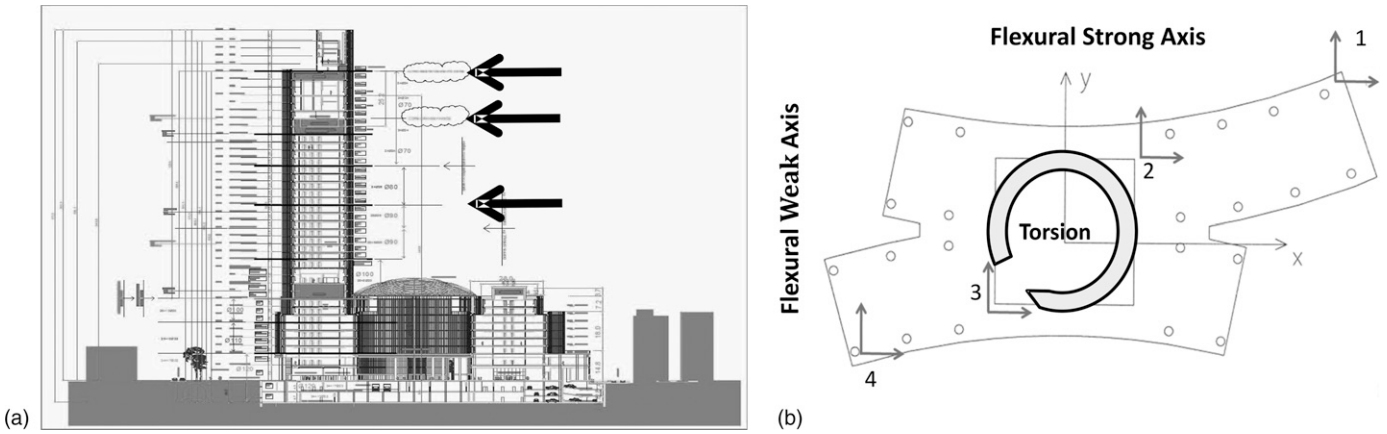

Fig. 10. Location of accelerometers: (a) lateral view; (b) floor plan of instrumented floors

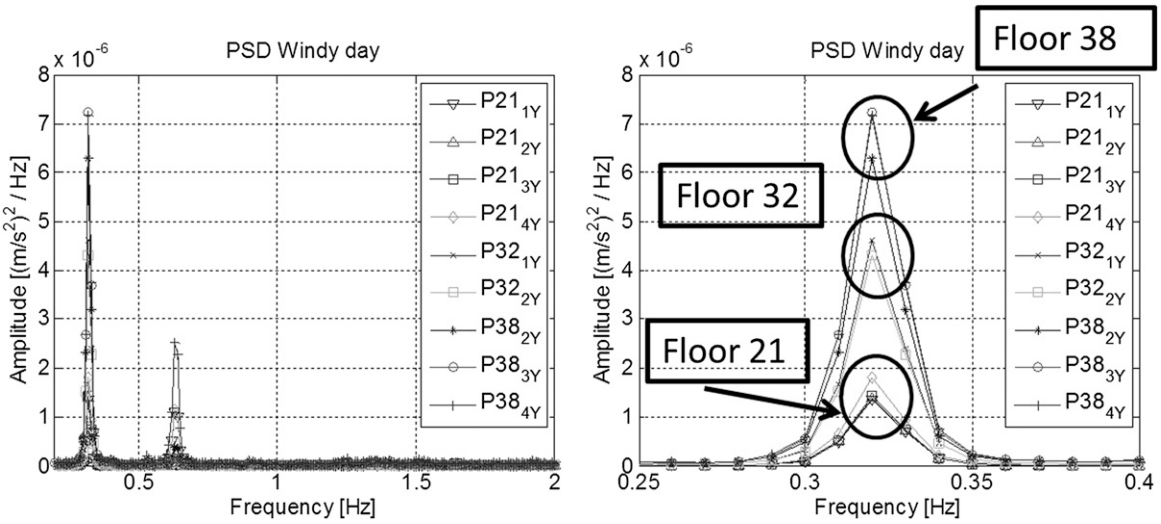

Fig. 11. Measured accelerations on a windy day: accelerometers located along the weak structural axis (21st, 32nd, and 38th floors)

frequencies only can be provided by means of long strokes and large masses.

To fulfill these requirements, a linear motor specifically adapted for the tests was lifted on top of Core 1 (38th floor), allowing movement up to 1,000 kg in the frequency range of interest, with a stroke close to 2 m. No other traditional means can provide the same performance. Fig. 12 shows the linear motor installed on the 38th floor.

Further, the possibilities given by the motor and the controlling unit allowed for a stepped sine testing with constant force amplitude on all the tested frequency range, resulting in two main advantages: (1) all the available energy was introduced at a single frequency and the response was measured at the same frequency, applying a synchronous-analysis approach that provides the best possible signal-to-noise ratio; (2) keeping the force amplitude constant on the whole frequency range reduces the nonlinear effects always present in these kinds of structures.

As previously stated, tests were carried out using a stepped sine excitation with a frequency resolution of 0.01–0.005 Hz, changed according to the known resonance positions (higher resolution close to resonance). The use of a stepped sine excitation allowed testing of

Fig. 12. Linear motor at 38th floor

the structure under steady-state conditions, thereby assuring maximum repeatability of the test results.

Measurements were analyzed through a synchronous approach to reduce spectral leakage. The acquired data were divided in a series of time windows containing an entire number of cycles at the forcing frequency, thereby assuring the minimum possible leakage in the frequency-response function estimation. An example of the identified frequency-response function is given in Fig. 13, in terms of amplitude and phase versus frequency, for the accelerations measured at the 38th floor. Positions refer to the points in Fig. 10. As can be seen in Fig. 13, the peaks identified via operational modal analysis are still present in the frequency-response function. Moreover, some resonances are evidenced in the 1.2–1.5 Hz area.

All the computed frequency-response functions were processed with the least-squares frequency-domain method (Peeters et al. 2004) to extract the relevant modal parameters. A summary of the identified modes in terms of frequency and damping is given in Table 2. Mode number three appears twice as it was identified during testing along both the strong and the weak flexural directions.

The identified damping values are compatible with those expected from the literature (Brownjohn 2007; Cigada et al. 2008a) considering the low-vibration amplitude. The values are slightly less than those obtained from operational modal analysis (Table 1), but this may be owing to the better signal-to-noise ratio of the forced test (Cattaneo et al. 2011).

The identified mode shapes are those expected from a cantilever beam; this aspect is discussed further in a numerical-experimental comparison.

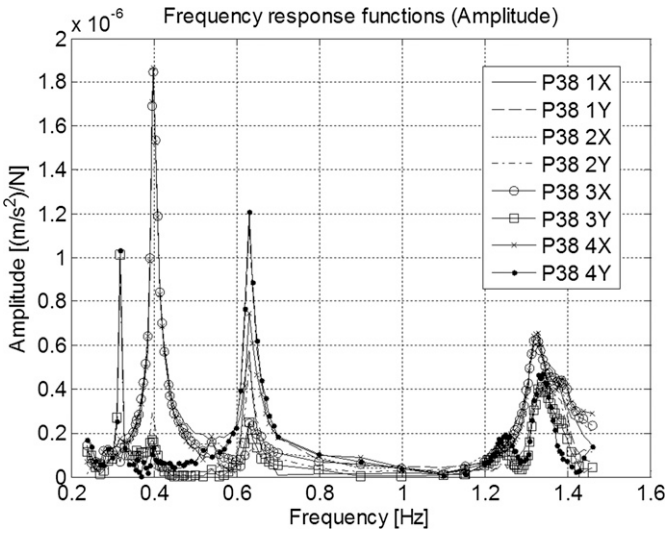

Fig. 13. Frequency-response function measured on 38th floor; excitation in the flexural strong-axis direction

Table 2. Identified Vibration Modes from the Forced Testing

Parameter	Mode 1	Mode 2	Mode 3	Mode 3	Mode 4	Mode 5
Frequency (Hz)	0.32	0.4	0.63	0.63	1.25	1.35
Damping (% RC)	1.19	1.47	1.49	1.43	1.46	1.28

Comparison and Discussion

The comparison between experimentally and numerically derived modal frequencies yielded good results, because of several reasons, mostly but not only related to the structural configuration.

From the structural design point of view, the basic conceptual design configuration of the structure was based on a uniform distribution of the load-bearing elements in the floor plan and on the reduction of differential lateral and vertical displacements of columns and core, meant to limit the negative effects of differential column shortening during the service life of the building.

The dynamic behavior of the structure is characterized by the first two mode shapes being almost totally uncoupled inflections along the two main stiffness axes, with no major torsional effects on the modal response and an almost completely uncoupled torsional third mode.

Also, a very strict quality-control procedure was carried out on both the materials and the construction methods; this was proven, for example, by the very good results of the strength tests on concrete cubes. For this reason, the nominal mechanical properties assumed in the design and modeling phases were very closely reflected in the as-built structure. Thus, when numerically computing the modal properties based on nominal material properties, no significant error would be generated.

From the numerical point of view, the model that took into account the stiffening effects of the columns on the slab elements gave a better prediction of the modal frequencies. In Tables 3 and 4, it can be seen that the rigid-joints model, as expected, improved the predicted frequencies, particularly in the weak direction (i.e., the second vibration mode), because the stiffening effect of the columns on the slabs was stronger in this direction. In both cases, though, the ratio of numerical versus experimental frequencies was in a range less than 1.10 for the first five modes (down to less than 1.05 for the first two modes), which is extremely good and particularly impressive for a model with this complexity and such a high number of degrees of freedom.

Table 3. Comparison between Numerical Analysis and Experimental Results: Modal Frequencies, No Rigid Joints

	Frequency (cycles/s)		
Mode	Measured	Numerical	Ratio measured/numerical
1	0.32	0.32	0.97
2	0.40	0.37	1.04
3	0.63	0.55	1.13
4	1.25	1.09	1.13
5	1.35	1.19	1.11

Table 4. Comparison between Numerical Analysis and Experimental Results: Modal Frequencies, Rigid Joints

	Frequency (cycles/s)		
Mode	Measured	Numerical	Ratio measured/numerical
2	0.32	0.34	0.95
3	0.40	0.40	0.99
4	0.63	0.57	1.11
5	1.25	1.12	1.11
5	1.35	1.24	1.08

As for the mode shapes, the eigenvectors exhibited full compatibility with the measured accelerations at the floors, in direction, proportion, and sign. This confirms a modal response dominated by the cantilever flexural mode along the weak axis (Mode 1, with almost

Table 5. Calculated MAC Values: Experimental versus Numerical Residues

MAC values (%)	Numerical mode number				
Experimental mode number	1	2	3	4	5
1	98	0	0	8	4
2	0	98	1	0	11
3	0	2	90	17	0
4	3	0	57	66	18
5	0	43	6	2	33

50% normalized participation factor), followed by a cantilever flexural mode along the strong axis (Mode 2, 42% normalized participation factor), and showing torsional effects only at higher modes.

Concerning the obtained mode shapes, a modal assurance criterion (MAC; Ewins 2001) analysis was carried out between the obtained numerical mode shapes and the correspondent experimental ones. MAC values were calculated among the modal residues extracted from the experimental analysis and the ones given by the numerical model in the same points where measurements were taken. The results of this analysis are given in Table 5.

As evident in Table 5, the MAC coefficient is very good for the first three modes, indicating a high degree of correlation between the experimental and numerical mode shapes. Concerning Mode 4, the degree of correlation is lower and some extra diagonal elements have values different from zero. The lower diagonal value is probably because of the lower vibration levels achieved for this mode (Fig. 13), and the extra diagonal values are due to the limited number of points used in the measurement mesh for this mode, which may lead to high correlation between different mode shapes. The MAC value for Mode 5 is quite low; but, if Fig. 13 is examined, Mode 5 is not clearly defined in the transfer function and this causes a higher uncertainty in the modal residue identification, even if the corresponding pole is identified clearly. Although the MAC coefficient calculated on this set of measurement points is not completely satisfactory, the good agreement found for the first three modes strengthens the good estimate obtained by the numerical model previsions.

Conclusions

This work reported on the dynamic behavior assessment of the Palazzo Lombardia tower in Milan. Both the main choices in numerical modeling and the experimental tests carried out to validate the model results were defined.

At first a description of the building was given, focusing on the strategic choices made during the design phase and in developing the numerical model. Then, the numerical model was explained, and, finally, the experimental campaign that was planned and carried out was presented.

The set of dynamic excitation tests conducted on Palazzo Lombardia proved to be an effective and reliable tool to validate the FE modeling assumptions and the basic conceptual choices enforced in the design phase.

The structural system exhibited a good response to dynamic excitation, governed by mostly uncoupled flexural deflection vibration modes associated with low frequencies, making it less sensitive to potential earthquake excitations.

The global numerical analysis model implemented in *GT STRUDL* proved to be well aligned with the basic parameters and assumptions and able to derive the modal properties of the structure with good accuracy. The experimental tests were an additional method used to enforce a final quality control on the materials and the construction method: they highlighted a good correspondence between the as-designed structure and the as-built one.

Thus, the numerical analysis model, experimentally validated, can now be used as the benchmark for the intended continuous monitoring activity of the Tower.

Acknowledgments

The authors acknowledge, for the help and the opportunity given, the following parties: Regione Lombardia (owner); Pei Cobb Freed & Partners Architects (USA) with Caputo Partnership (Italy) and Sistema Duemila (Italy), Architectural Project Supervisor Henry N. Cobb (architectural designers); Infrastrutture Lombarde Spa (construction supervisor); Consorzio Torre Spa (general contractor); Impregilo Spa, President and General Manager Gaetano Salonia (lead contractor); Vinicio Scerri (site technical manager); and Guglielmo Fariello (construction site general manager and safety supervisor).

References

Bendat, J. S., and Piersol, A. G. (2000). *Random data: Analysis and measurement procedures*, 3rd Ed., Wiley-Blackwell, Hoboken, NJ.

British Standards Institution (BSI). (1990). *BS EN 1990 Eurocode 0: Basis of structural design,* London.

Brownjohn, J. M. W. (2007). "Structural health monitoring of civil infrastructure." *Philos. Trans. R. Soc. London, Ser. A*, 365(1851), 589–622.

Canadian Commission on Building and Fire Codes. (2006). *User's Guide–NBC 2005: Structural Commentaries (Part 4 of Division B)*, National Research Council Canada, Institute for Research in Construction, Ottawa, ON, Canada.

Caprioli, A., Cigada, A., Gentile, C., and Vanali, M. (2009) "Comparison of two different OMA techniques applied to vibration data measured on a Stadium grandstand." *Proc., Int. Conf. IOMAC '09—3rd Int. Operational Modal Analysis Conf.*, Univ. of Minho, Guimarães, Portugal, 81–87.

Carden, E. P. (2004). "Vibration based condition monitoring: A review." *Struct. Health Monit.*, 3(4), 355–377.

Cattaneo, A., Manzoni, S., and Vanali, M. (2010). "Measurement uncertainty in operational modal analysis of a civil structure." *Proc., Int. Conf. on Uncertainty in Structural Dynamics*, KU Leuven, Leuven, Belgium, 5103–5116.

Cattaneo, A., Manzoni, S., and Vanali, M. (2011). "Numerical investigations on the measurement uncertainty in operational modal analysis of a civil structure." *Proc., Int. Conf. IMAC XXIX,* Society for Experimental Mechanics, Bethel, CT.

Cigada, A., Caprioli, A., Redaelli, M., and Vanali, M. (2008a). "Numerical modeling and experimental modal analysis of a concrete grand-stand structure to structural health monitoring purposes." *Proc., Int. Conf. IMAC XXVI,* Society for Experimental Mechanics, Bethel, CT.

Cigada, A., Caprioli, A., Redaelli, M., and Vanali, M. (2008b). "Vibration testing at Meazza Stadium: Reliability of operational modal analysis to health monitoring purposes." *J. Perform. Constr. Facil.*, 10.1061/(ASCE)0887-3828(2008)22:4(228), 228–237.

Cigada, A., Caprioli, A., Redaelli, M., and Vanali, M. (2008c). "Long term monitoring of the G. Meazza stadium in Milan, from the first measurements to the permanent monitoring system installation." *Proc., Int. Conf. Eurodyn*, Southampton, U.K.

Cigada, A., Mola, E., Mola, F., Stella, G., Vanali, M., and Zappa, E. (2011). "L'importanza del collaudo dinamico delle strutture." *Tutto Misure*, 44(11), 277–280 (in Italian).

Cigada, A., Moschioni, G., Vanali, M., and Caprioli, A. (2010). "The measurement network of the San Siro Meazza Stadium in Milan: Origin and implementation of a new data acquisition strategy for structural health monitoring." *Exp. Tech.*, 34(1), 70–81.

Consiglio Superiore dei Lavori Pubblici. (2008). *Nuove Norme Tecniche per le Costruzioni, DM 14-01-08*, Rome (in Italian).

Cornwell, P. J., Farrar, C. R., Doebling, S. W., and Sohn, H. (1999). "Environmental variability of modal properties." *Exp. Tech.*, 23(6), 45–48.

Council of Tall Buildings and Urban Habitat (CTBUH). (2014). "CTBUH height criteria." ⟨http://www.ctbuh.org/TallBuildings/HeightStatistics/Criteria/tabid/446/language/en-US/Default.aspx⟩ (Mar. 13, 2014).

D'Antona, G., and Ferrero, A. (2006). *Digital signal processing for measurement systems: Theory and applications (information technology: transmission, processing and storage)*, Springer, New York.

Doebling, S. W., Farrar, C. R., and Prime, M. B. (1998). "A summary review of vibration-based damage identification methods." *Shock Vib. Digest*, 30(2), 91–105.

Doebling, S. W., Farrar, C. R., Prime, M. B., and Shevitz, D. W. (1996). "Damage identification and health monitoring of structural and mechanical systems from changes in their vibration characteristics: A literature review." *Rep. LA-13070-MS,* Los Alamos National Laboratory, Los Alamos, NM.

El-Kafafy, M., Guillaume, P., Peeters, B., Marra, F., and Coppotelli, G. (2012). "Advanced frequency-domain modal analysis for dealing with measurement noise and parameter uncertainty." *Proc., Int. Conf. IMAC XXX*, Society for Experimental Mechanics, Bethel, CT, 179–202.

Ewins, J. (2001). *Modal testing: Theory, practice and application*, 2nd Ed., Taylor & Francis Group, London.

Fan, W., and Qiao, P. (2010). "Vibration-based damage identification methods: A review and comparative study." *Struct. Health Monit.*, 10(1), 83–111.

Farrar, C. R. (1997). "System identification from ambient vibration measurements on a bridge." *J. Sound Vib.*, 205(1), 1–18.

Fédération International de la Précontrainte (CEB/FIP). (1993). "Structural effects of time-dependent behaviour of concrete." *Bulletin No. 215,* Paris.

GT STRUDL 30 [Computer software]. Huntsville, AL, Intergraph.

Huth, O., Feltrin, G., Maeck, J., Kilic, N., and Motavalli, M. (2005). "Damage identification using modal data: Experiences on a prestressed concrete bridge." *J. Struct. Eng.*, 10.1061/(ASCE)0733-9445(2005)131:12(1898), 1898–1910.

Institution of Structural Engineers. (2008). *Dynamic performance requirements for permanent grandstands subject to crowd action: Recommendations for management design and assessment*, London.

ISO. (1997). "Mechanical vibration and shock – Evaluation of human exposure to whole-body vibration – Part 1: General requirements." *2631-1:1997,* Geneva.

ISO. (2003). "Mechanical vibration and shock – Evaluation of human exposure to whole-body vibration – Part 2: Vibration in buildings." *2631-2:2003,* Geneva.

Mohanty, P., and Rixen, D. J. (2004). "Operational modal analysis in the presence of harmonic excitation." *J. Sound Vib.*, 270(1–2), 93–109.

Mola, F. (2010). "The Altra Sede building for the Regione Lombardia in Milan: Conceptual design and technological features of the tallest building in Italy." *Proc., IABSE Symp. 2010*, International Association for Bridge and Structural Engineering, Zurich, Switzerland.

Peeters, B., Van der Auweraer, H., Guillaume, P., and Leuridan, J. (2004). "The PolyMAX frequency-domain method: A new standard for modal parameter estimation?" *Shock Vib.*, 11(3–4), 395–409.

Peeters, B., Vanhollebeke, H., and Van der Auweraer, H. (2005). "Operational PolyMAX for estimating the dynamic properties of a stadium structure during a football game." *Proc., Int. Conf. IMAC XXIII*, Society for Experimental Mechanics, Bethel, CT.

Pintelon, R., Guillaume, P., and Schoukens, J. (2007). "Uncertainty calculation in (operational) modal analysis." *Mech. Syst. Signal Process.*, 21(6), 2359–2373.

Salawu, O. S. (1997). "Detection of structural damage through changes in frequency: A review." *Eng. Struct.*, 19(9), 718–723.

Sohn, H., et al. (2004). "A review of structural health monitoring literature: 1996–2001." *Rep. LA-13976-MS*, Los Alamos National Laboratory, Los Alamos, NM.

Teughels, A., and De Roeck, G. (2004). "Structural damage identification of the highway bridge Z24 by FE model updating." *J. Sound Vib.*, 278(3), 589–610.

Vanali, M., and Cigada, A. (2009). "Long term operational modal analysis of a stadium grandstand to structural health monitoring purposes." *Proc., IEEE Workshop on Environmental, Energy, and Structural Monitoring Systems,* IEEE, New York, 103–109.